Available online at www.eccomasproceedia.org
Eccomas Proceedia COMPDYN (2023) 2841-2856

ECCOMAS
Proceedia

COMPDYN 2023
9th ECCOMAS Thematic Conference on
Computational Methods in Structural Dynamics and Earthquake Engineering
M. Papadrakakis, M. Fragiadakis (eds.)
Athens, Greece, 12-14 June 2023

PRELIMINARY RESULTS OF A SHAKING-TABLE DYNAMIC TEST ON A REPAIRED AND ENHANCED REINFORCED CONCRETE INFILLED STRUCTURE

Riccardo R. Milanesi[1], Gabriele Guerrini[2], Davide Bolognini[1], Luca Grottoli[1], Filippo Dacarro[1], Paolo Morandi[1]

[1] EUCENTRE Foundation
Via Ferrata, 1 - 27100, Pavia (PV) - Italy
{riccardo.milanesi, davide.bolognini, luca.grottoli, filippo.dacarro, paolo.morandi}@eucentre.it

[2] Department of Civil Engineering and Architecture
University of Pavia
Via Ferrata, 3 - 27100, Pavia (PV) - Italy
gabriele.guerrini@unipv.it

Abstract

Although several post-earthquake surveys and previous studies have addressed the seismic vulnerability of infilled reinforced concrete (RC) structures built without proper seismic design, investigations have focused on repair and enhancement techniques only in recent years thanks to the development of new materials and the increase of public awareness. Moreover, experimental investigations have more commonly addressed strengthening techniques of pristine specimens rather than repairing solutions for damaged elements, because of the difficulty in defining a proper level of pre-existing damage.

This paper describes an experimental campaign conducted at the EUCENTRE Foundation (Pavia, Italy) and discusses some preliminary results. The research work addresses the effectiveness of repair and strengthening techniques applied to a pair of identical structures through incremental dynamic shake-table tests. The specimens consisted of real scale three-story RC frames with clay masonry infills that were previously damaged up to two different levels to simulate two distinct post-earthquake conditions.

The structures were repaired and enhanced depending on the preexisting damage and then subjected to the same loading protocol to allow a direct comparison on the effectiveness of the adopted techniques. The interventions involved the most vulnerable structural and non-structural elements and can be summarized in: (i) strengthening of the first-story RC columns, (ii) repair and enhancing of first-story RC slab-column joints, and (iii) enhancement of the masonry infills for both in-plane and out-of-plane resistance.

Keywords: existing reinforced concrete frames, masonry infills, seismic repair, seismic strengthening, dynamic shake-table test.

ISSN:2623-3347
Peer-review under responsibility of the organizing committee of COMPDYN 2023.
doi: 10.7712/120123.10604.21164

1 INTRODUCTION

Infilled reinforced concrete (RC) frames are among the most common structural typology in many countries worldwide: they have become popular during the XX century and are still frequently built. The knowledge acquired through post-earthquake field observations [1-2] or experimental and numerical scientific studies [3-12] has led to progressive improvements in the response of these structures, especially thanks to code prescriptions addressing new construction. However, a large number of existing buildings that were not designed for earthquake resistance are still in use, and are typically affected by severe damage in seismic events (Figure 1).

Despite the well-known deficiencies causing the seismic vulnerability of infilled RC structures, investigations have focused on repair and enhancement techniques only in recent years, thanks to the sharp evolution of the construction material industry and to the increased public awareness about seismic risk mitigation [11-12]. Strengthening techniques have usually been studied through separate experimental investigations to characterize, for example, the enhancement on RC column or beam elements [13-17], RC beam-column joints [18-19], or masonry infills [20-28]. Experimental studies more commonly address interventions applied to pristine specimens than repairing techniques for damaged elements, due to the difficulty in defining a proper level of pre-existing earthquake damage.

This work discusses the seismic behavior of a pair of real scale three-story infilled RC frames, considering the preliminary results of a unidirectional dynamic shake-table test and focusing on the effectiveness of repair and strengthening interventions applied to columns, slab-column joints, and infill walls. The two structures were identical except for the level of initial damage; in fact, they were previously tested on a different experimental campaign that induced severe damaged on one specimen, but only minor damage on the other one [29].

(a) (b)

Figure 1 Damage to infilled frames and RC elements after the 2016 Central Italy earthquake sequence: (a) infill panels; (b) RC beam-column joint.

2 DESCRIPTION OF THE SPECIMENS AND INTERVENTIONS

2.1 Original structures from the previous experimental campaign

The original structures were part of a previous experimental campaign [29]. The two test specimens (Figure 2) consisted of two three-dimensional infilled RC frames, with 4 columns each. Each building had a floor plan of 5.0 m x 2.1 m and clear story heights of 2.5 m. They were built side by side on the same RC foundation, fastened to the shaking table, leaving a gap of about 20 cm orthogonal to the shaking direction.

The RC columns had a 20 cm x 20 cm square cross-section. They were reinforced with 4 Φ16-mm longitudinal corner bars (with a reinforcement ratio of about 2%) and Φ8-mm closed square stirrups spaced at 100 mm (Figure 3). At the lower and upper ends of the first-story columns the stirrup spacing was reduced to 50 mm over a length of about 400 mm. The floors consisted of 400-mm-thick solid RC slabs. No stirrups or other shear reinforcement was provided at the slab-column joints within the slab thickness, to simulate non-seismic detailing.

9-cm-thick infills were provided within the 6 longitudinal bays (2 per floor) of each frame. They consisted of 8-cm-thick, hollow clay units with holes aligned horizontally and an about 65% perforation rate. An approximately 1-cm-thick plaster layer was applied on one side of the panels, using the same mortar of the infill bed joints. The internal infills at the first and second stories had respectively 3 and 2 openings of different sizes, to accommodate the elements of a safety steel frame; the external infills had identical perforations at the same stories to grant symmetry.

At the end of the previous testing campaign, the first-story RC joints and infills of the West building were heavily damaged (Figure 4), after reaching a peak interstory drift ratio of 0.88%.

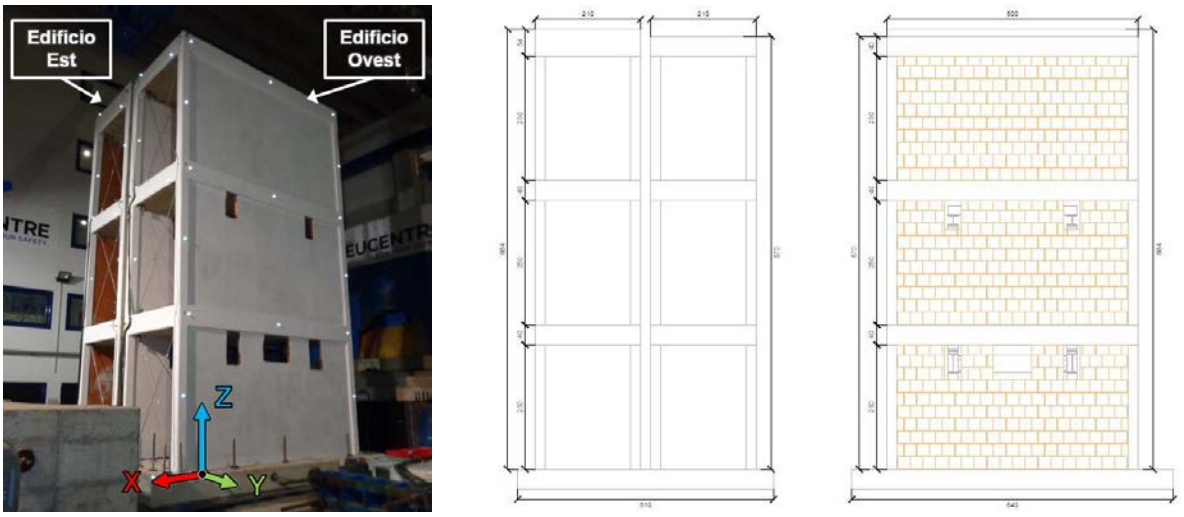

(a) (b) (c)

Figure 2 Specimens from the previous experimental campaign: (a) North-West corner photo; (b) North elevation; (c) West elevation [29].

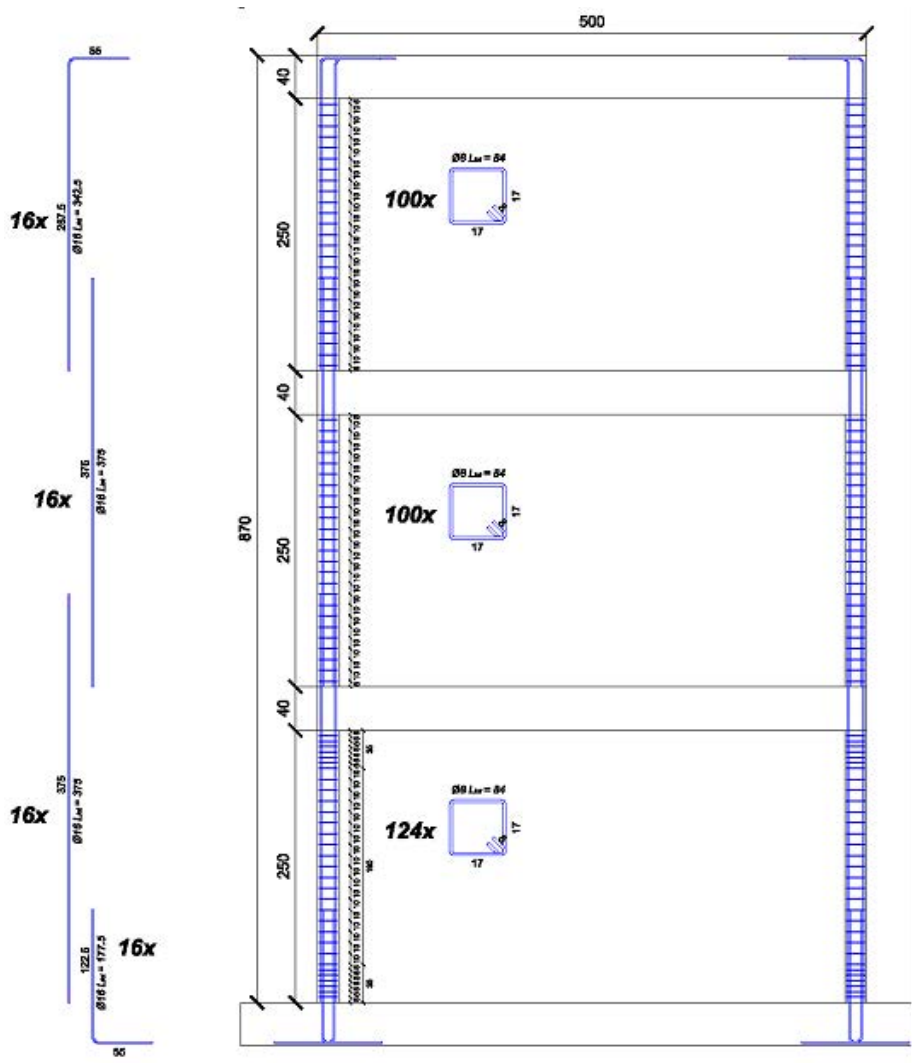

Figure 3 Column reinforcement details of the original RC structure.

(a) (b)

Figure 4 Damage at the end of the previous experimental campaign before interventions: (a) infill panels; (b) RC beam-column joint.

2.2 Interventions on RC members and masonry infills

The extent of damage found in both buildings at the end of the previous experimental campaign was comparable to situations that occur after a high-intensity seismic event. Such damage provided an ideal context for testing repair solutions and strengthening techniques on RC structural elements and masonry infills. Therefore, the following activities were carried out:

1. Demolition of the first-story masonry infills of both buildings;
2. Repair and strengthening of the first-story RC columns and slab-column joints of both structures with a high-performance, fiber-reinforced concrete jacket (Figure 5);
3. Reconstruction of the first-story masonry infills of both specimens, avoiding openings on the exterior panels, where not required by the steel safety frame (Figure 6a);
4. In-plane enhancement of all masonry infills, except for the two first-story panels of the East building (Figure 6b-c), by applying a basalt-fiber mesh within a specific mortar;
5. Construction of 4 double-leaf masonry infills (2 per building) at the second story and of 6 infills (3 per building) at the third story, perpendicular to the shaking direction, to be tested out of plane (Figure 7); these panels had a length of about 1.0 m, were restrained only at their top and bottom, and were left free along their vertical edges;
6. Enhancement of the out-of-plane masonry panels through several techniques, including (i) fastening to the top RC slab, (ii) adding rigid or flexible connections between the two masonry leaves, and (iii) providing different surface enhancements such as the application of a particular mortar on one or both sides, with or without a basalt-fiber mesh.

(a) (b) (c) (d)

Figure 5 Interventions on RC frame: (a) first-story beam-column joint of the East building at the end of the previous experimental campaign; (b) joint repairing; (c) column strengthening; (d) cross-section of the strengthened column during the demolition at the end of the tests.

(a) (b) (c)

Figure 6 Interventions on masonry infills: (a) first-story infill reconstruction; (b) in-plane infill enhancement with basalt-fiber mesh and mortar; (c) in-plane enhanced infill after completion.

(a) (b)

Figure 7 Masonry panels for out-of-plane testing: (a) construction of a double-leaf panel; (b) plastered panel before enhancement.

3 TEST SETUP, PROTOCOL, AND INSTRUMENTATION

In the chosen reference system, the northward X-axis coincides with the shaking direction, while the Y- and Z-axis point westward and upward, respectively (Figure 2). In its final configuration, the specimens consisted of two RC frames with masonry infills in the longitudinal (X) direction, both resting on the same foundation slab anchored to the shaking table. Therefore, the same unidirectional acceleration histories were applied along the X-axis to both buildings simultaneously during the tests.

One horizontal component of the November 23rd, 1980, Irpinia (Italy) earthquake was selected as the input signal and applied incrementally, with random noise run between each increment for dynamic identification and control calibration purposes. The original ground motion record is characterized by peak ground acceleration PGA = 0.32 g, effective duration T_D = 6.32 s, Arias intensity I_a = 1.41 m/s, and cumulative absolute velocity CAV = 10.88 m/s. Figure 8 shows the ground motion signal and its acceleration spectrum for 5% damping. Table 1 reports the nominal and actual PGA and maximum spectral accelerations.

Accelerometers and displacement transducers were installed to monitor the global response of the structures and the local behavior of the panels excited out of their planes. The two buildings were equipped with the same sensor layout, for a total of 27 accelerometers and 47 linear displacement transducers (Table 2).

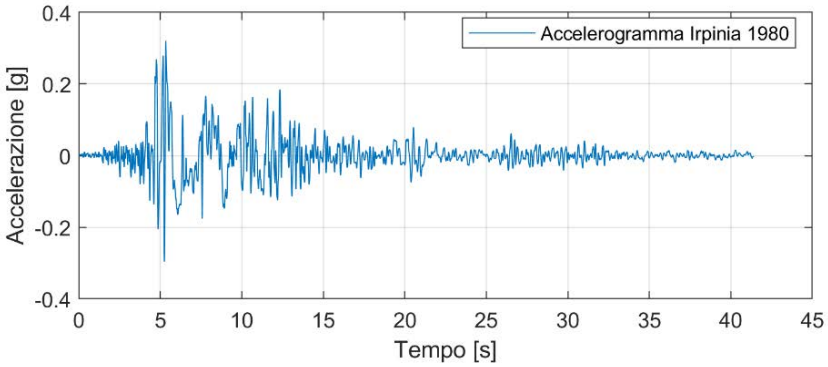

(a)

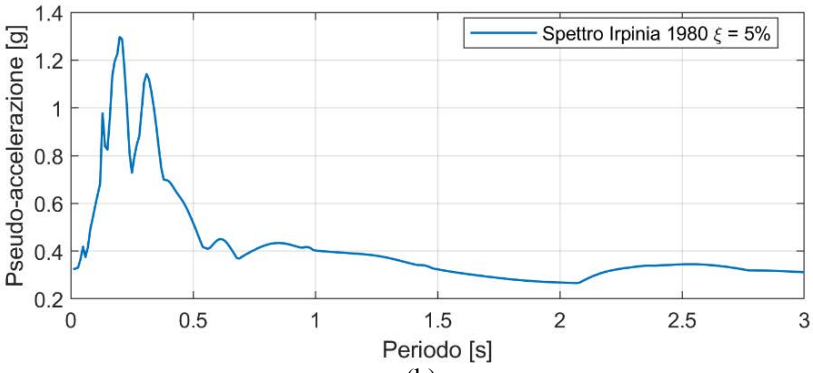

(b)

Figure 8 Irpinia 1980 earthquake: (a) reference time history ground motion; (b) spectrum at 5% damping.

Test No.	PGA (nominal) [g]	PGA (actual) [g]	Max spectral acceleration (nominal) [g]	Max spectral acceleration (experimental) [g]
2	0.08	0.06	0.33	0.15
3	0.08	0.08	0.33	0.27
4	0.08	0.09	0.33	0.29
6	0.32	0.22	1.31	0.66
8	0.32	0.36	1.31	1.06
10	0.32	0.42	1.31	1.42
12	0.40	0.58	1.64	1.84
14	0.48	0.79	1.97	2.36
17	0.56	0.41	2.30	1.24
18	0.56	0.35	2.30	1.27
20	0.40	0.49	1.64	1.60

Table 1 Main test sequence and input accelerations.

Accelerometers	
2	Shaking table and RC foundation
12	2 per floor on each structure
5	Setup elements where linear transducers were installed
8	Centre of each out-of-plane infill at the second story
Linear displacement transducers	
4	Relative displacement and uplift between the shaking table and the RC foundation
1	Displacement of the shaking table
24	Displacement and rotation of the floor slabs
18	Displacements of the out-of-plane infill panels (3 per panel)

Table 2 Accelerometers and linear displacement transducers.

4 PRELIMINARY EXPERIMENTAL RESULTS

The great quantity of testing data provides both general and specific outcomes, dealing with the overall behavior of the structure and the seismic response of individual structural members and enhanced masonry infills. Furthermore, the comparison with the unstrengthened building tested in the previous experimental campaign allows for an interesting discussion. However, most of the results require a deeper interpretation that will be part of future work. In this section, the preliminary results are only briefly reported.

4.1 Damage evolution during the test

The damage evolution highlighted an overall satisfiying seismic response of the infilled structure, with evident effectiveness of the first-story RC column and joint repair/strengthening resulting in a soft-story mechanism at the unstrenghetend second storey in both structures. The main structural damage occurred at the second floor RC non-retrofitted slab-column joints (Figure 9).

The enhanced infills successfully reached a 1.20% peak interstory drift ratio with only localized and repairable damage (Figure 10). The improved panels also showed a superior out-of-plane behavior compared to the unstrengthened ones, although their detailed behavior will be addressed in future publications.

Table 3 summarizes the main aspects of the damage pattern.

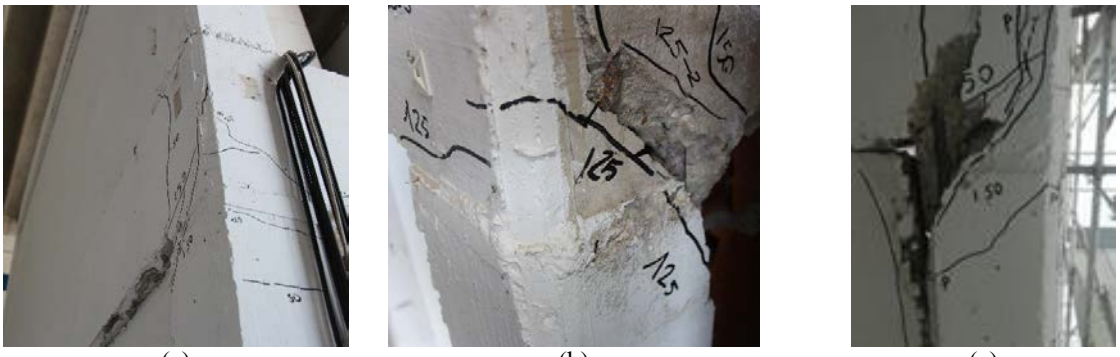

(a) (b) (c)

Figure 9 Damage evolution of the unstrengthened second-floor slab-column joints: (a) after test 14; (b) after test 18; (c) after test 20.

(a) (b) (c)

Figure 10 Damage evolution of the infills excited in their plane: (a) after test 12; (b) after test 14; (c) after test 18.

Test No.	PGA [g]	RC structures	Infills excited in plane
4	0.09	Flexural cracks on the 2nd-story columns.	Small cracks at the interface between all infills and RC elements.
6	0.22	Increased number/length of existing cracks. Shear cracks in the 2nd-floor slab-column joints of the West frame.	Cracks almost all along the 2nd- and 3rd-story infill interfaces. Unstrengthened 1st-story infills almost detached from the RC frame, yet stable.
8	0.36	Increased number/length of existing cracks. Flexural cracks along the 3rd-story columns.	Cracks all along the interfaces of all infills. Crushing of the top-north corner masonry unit of the 2nd-story West infill of the West frame.
10	0.42	Increased number/length of existing cracks. Cracks at the bottom of the 2nd-story slab near the columns of the West frame.	Increased width of interface cracks. Diagonal crack in the 1st-story unstrengthened infill between opening and top corner. Minor corner detachments of the strengthening plaster at the 2nd story.
12	0.58	Increased number/length of existing cracks. Flexural cracks along the 1st-story columns. Shear cracks in the 2nd- and 3rd-floor slab-column joints of the East frame.	Diagonal crack in the 1st-story enhanced infill between opening and top corner. Still limited corner detachments of the strengthening plaster (Figure 10a), now also at the 1st story.
14	0.79	Increased number/length of existing cracks. Considerable shear cracks in the 2nd-story joints (Figure 9a). Small flexural cracks on the 1st-floor slab side, close to the strengthened nodes.	Increased cracking on the 1st-story unstrengthened infill with openings (Figure 10b). Cracking of the 2nd-story strengthened infill with openings. Increased corner detachments of the strengthening plaster at the 2nd story.
17 18	0.41 0.35	Increased number/length of existing cracks. Spalling in the 2nd-story joints on the North sides of both frames (Figure 9b).	Increased cracking on the 1st-story unstrengthened infill with openings. Increased corner detachments of the strengthening plaster at the 2nd story, with masonry crushing of a few top corners in the West building (Figure 10c).
20	0.49	Increased number/length of existing cracks. Extensive spalling in the 2nd-story joints on the North sides of both frames (Figure 9c).	General worsening of existing damage patterns. Crushing of the top-north corner masonry unit of the 1st-story East infill of the East frame.

Table 3 Summary of the damage evolution on RC elements and infills excited in plane.

4.2 Preliminary plots of the experimental results

The global results for the two infilled structures have been derived from the instrumentation installed on the slabs. The acceleration, force, and displacement values are taken along the X-axis, i.e. the shaking direction of the unidirectional test sequence.

Figure 11 shows the positive and negative floor acceleration envelopes for every test. In Table 4 and Table 5 also the peak floor accelerations are reported, together with the corresponding amplifications with respect to the applied table accelerations.

The positive and negative floor displacement envelopes are plotted in Figure 12 for every test. The interstory displacements concentrate at the second story, were peak interstory drift ratios of 1.0% and 1.2% were reached in the East and West building, respectively. The maximum first-story drift ratios were at 0.32% and 0.19% for the same buildings, whereas the second-story ratios peaked at 0.24% and 0.22%.

Test No.	Maximum floor acceleration [g]				Accel. amplification w.r.t table [-]		
	Table	Floor 1	Floor 2	Floor 3	Floor 1	Floor 2	Floor 3
2	0.059	0.070	0.087	0.095	1.192	1.479	1.607
3	0.085	0.113	0.158	0.160	1.341	1.863	1.885
4	0.094	0.157	0.199	0.198	1.673	2.121	2.101
6	0.215	0.366	0.501	0.633	1.701	2.331	2.940
8	0.356	0.624	0.887	1.014	1.752	2.487	2.846
10	0.424	0.741	1.188	1.233	1.745	2.799	2.906
12	0.583	0.761	1.311	1.327	1.305	2.248	2.276
14	0.894	0.951	1.309	1.430	1.197	1.649	1.801
17	0.408	0.630	1.063	1.162	1.546	2.607	2.851
18	0.349	0.666	0.975	1.174	1.907	2.790	3.362
20	0.491	0.933	1.127	1.373	1.901	2.296	2.797

Table 4 Maximum floor accelerations and amplifications of the East building.

Test No.	Maximum floor acceleration [g]				Accel. amplification w.r.t. table [-]		
	Table	Floor 1	Floor 2	Floor 3	Floor 1	Floor 2	Floor 3
2	0.059	0.066	0.103	0.120	1.125	1.741	2.042
3	0.085	0.131	0.182	0.214	1.543	2.153	2.531
4	0.094	0.150	0.219	0.272	1.591	2.328	2.890
6	0.215	0.417	0.496	0.675	1.936	2.306	3.138
8	0.356	0.590	0.799	1.067	1.654	2.241	2.993
10	0.424	0.707	1.113	1.363	1.666	2.623	3.210
12	0.583	0.941	1.415	1.504	1.614	2.428	2.508
14	0.894	1.089	1.265	1.430	1.372	1.593	1.801
17	0.408	0.664	1.183	1.322	1.630	2.903	3.242
18	0.349	0.698	1.145	1.235	1.999	3.278	3.534
20	0.491	0.915	1.225	1.299	1.865	2.495	2.645

Table 5 Maximum floor accelerations and amplifications of the West building.

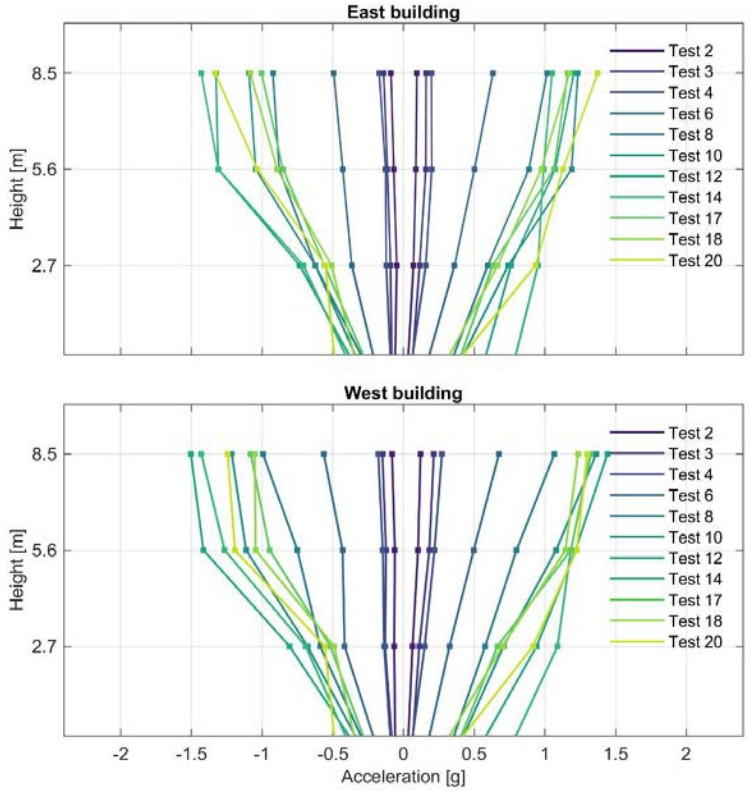

Figure 11 Positive and negative floor acceleration envelopes for both buildings and every test.

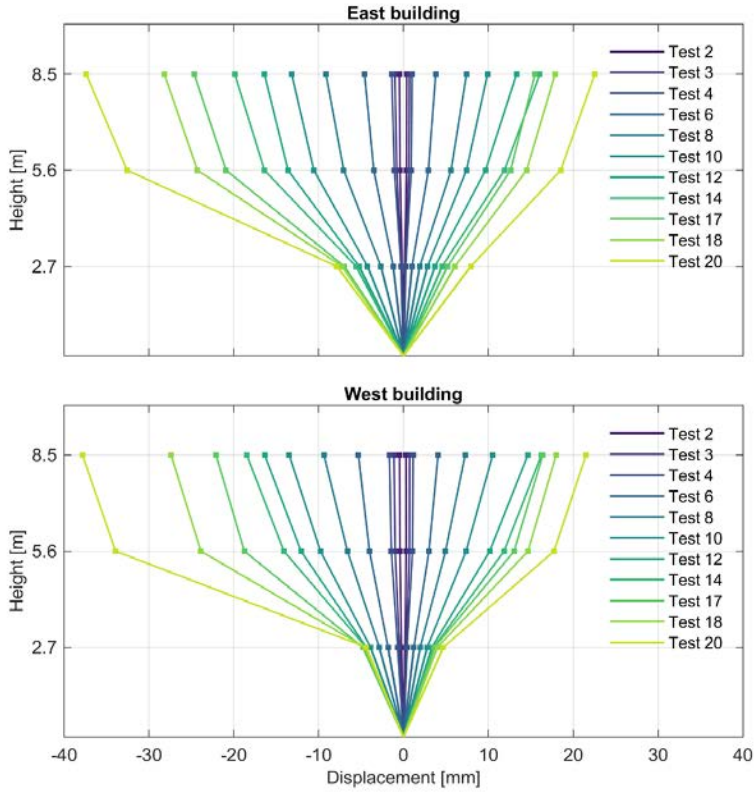

Figure 12 Positive and negative displacement envelopes for both buildings and every test.

Floor inertia forces were calculated by multiplying floor accelerations times tributary masses, according to Figure 13**Errore. L'origine riferimento non è stata trovata.**a. The shear-displacement backbone curves were plotted in terms of both global response (base shear vs top displacement, Figure 13**Errore. L'origine riferimento non è stata trovata.**b) and individual story response (story shear vs. interstory displacement, Figure 13**Errore. L'origine riferimento non è stata trovata.**c). These curves were obtained by taking the points of maximum positive and negative shear from each test run.

The specimens behaved similarly overall, with the East building showing slightly larger deformation of the first story (whose slab-column joints, even though repaired, were previously severely damaged) while the West building concentrating more at the second story.

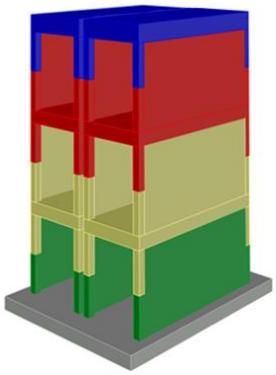

(a)

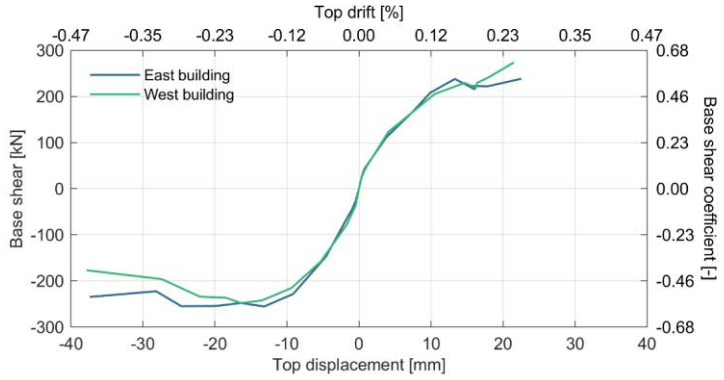

(b)

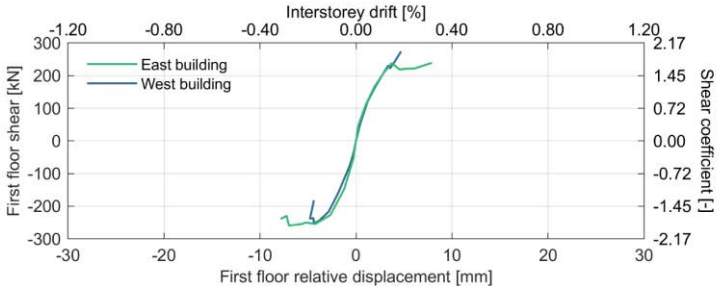

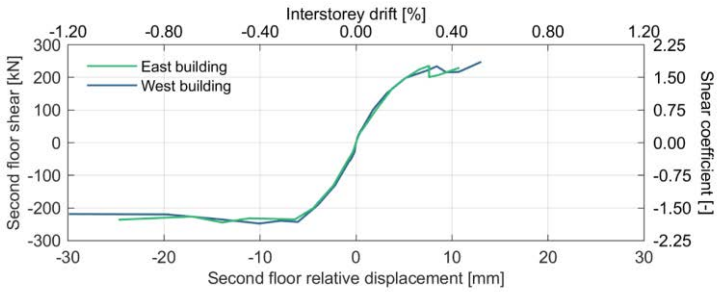

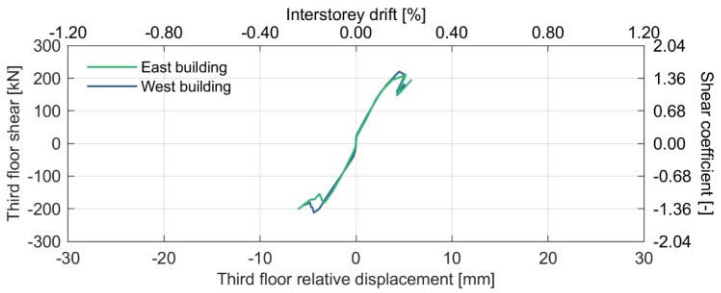

(c)

Figure 13 Lateral force-displacement responses: (a) mass distribution for the computation of inertia forces; (b) base shear vs. top displacement backbone curves; (c) individual story shear vs. interstory drift backbone curves.

5 CONCLUSIONS

The experimental study discussed in this paper is the continuation of a previous campaign [29] where two identical infilled RC structures were damaged to different extents through a unidirectional dynamic shake-table test, with a natural ground motion record applied in incremental steps. The two specimens, consisting of one-bay, three-story RC frames, were built at real scale, side by side on the same foundation. The masonry infills were made of hollow clay units with holes aligned horizontally.

For this work, the damaged structures were repaired (first-story RC slab-column joints) and strengthened (first-story RC joints and columns) with a high-performance, fiber-reinforced concrete jacket. The masonry infills parallel to the shaking direction were rebuilt at the first story and enhanced with a basalt-fiber mesh embedded in a plaster overlay, everywhere except for the first story of one building. Some infill panels were also built and strengthened perpendicular to the shaking direction, but their out-of-plane behavior is not the object of this paper.

The damage evolution, the floor acceleration and displacement envelopes, and the story shear-displacement backbone curves demonstrate an improved seismic performance of the structural and non-structural elements that had been repaired and/or enhanced. The failure mechanism transitioned from a soft first story (previous campaign) to a soft second story, controlled by shear on the unstrengthened second-floor slab-column joints. Indeed the interventions on the first-floor RC joints not only restored their original resistance, but also effectively increased it, making then stronger than the second-floor ones. Furthermore, the in-plane drift imposed on the enhanced infills at the second story demonstrated their increased deformation capacity, compared to the bare masonry ones.

This paper presents only the preliminary results of the experimental campaign, and future developments will cover several aspect such as a complete comparison with the unstrengthened infilled structure previously tested, a more detailed interpretation of the repair/strengthening effects on the global infilled frame response and on the in-plane infill behavior [28], and an analysis of the out-of-plane infill response with different enhancement interventions.

ACKNOWLEDGEMENTS

The work presented is part of an ongoing study at the EUCENTRE Foundation in collaboration with Kerakoll S.p.A., that is acknowledged for its financial support.

REFERENCES

[1] A. Masi, L. Chiauzzi, G. Santarsiero, V. Manfredi, S. Biondi, E. Spacone, C. Del Gaudio, P. Ricci, G. Manfredi, G.M. Verderame. Seismic response of RC buildings during the Mw 6.0 August 24, 2016 Central Italy earthquake: the Amatrice case study. *Bull Earthquake Eng*, 17, 5631–5654, https://doi.org/10.1007/s10518-017-0277-5, 2019.

[2] I.O. Demirel, A. Yakut, B. Binici, Seismic performance of mid-rise reinforced concrete buildings in Izmir Bayrakli after the 2020 Samos earthquake, *Engineering Failure Analysis*, 137, 106277, https://doi.org/10.1016/j.engfailanal.2022.106277, 2022.

[3] R.E. Klingner, N.R. Rubiano, T.R. Bashandy, S.C. Sweeney, Evaluation and analytical verification of shaking table data from infilled frames, *11th World Conference on Earthquake Engineering*, Acapulco, Mexico, June 23-28, 1996.

[4] A. Hashemi, K.M. Mosalam, Shake-table experiment on reinforced concrete structure containing masonry infill wall, *Earthquake Engineering and Structural Dynamics*, 35: 1827-1852, 2006.

[5] A. Stavridis, I. Koutromanos, P.B. Shing, Shake-table tests of a three-story reinforced concrete frame with masonry infill walls, *Earthquake Engineering and Structural Dynamics,* 41: 1089-1108, 2012.

[6] M. Tondelli, S. Petry, S. Peloso, K. Beyer, Shake-table test on four-storey structure with reinforced concrete and unreinforced masonry walls, *Proc. Recent Advances in Earthquake Engineering and Strucrural Dynamics 2013*, Vienna, Austria, August 28-30, 2013.

[7] M. Tondelli, S. Petry, I. Lanese, S. Peloso, K. Beyer. Shake Table Testing of a Half-Scaled RC-URM Wall Structure. *In: Taucer, F., Apostolska, R. (eds) Experimental Research in Earthquake Engineering. Geotechnical, Geological and Earthquake Engineering*, vol 35. Springer, Cham. https://doi.org/10.1007/978-3-319-10136-1_18, 2015.

[8] G.J. O'Reilly, T.J. Sullivan. Modeling Techniques for the Seismic Assessment of the Existing Italian RC Frame Structures, *Journal of Earthquake Engineering*, DOI: 10.1080/13632469.2017.1360224, 2017.

[9] G.M. Verderame, P. Ricci, M.T. De Risi, C. Del Gaudio, Experimental Assessment and Numerical Modelling of Conforming and Non-Conforming RC Frames with and without Infills, *Journal of Earthquake Engineering*, 26(2), 573-614, 2022.

[10] M.T. De Risi, M. Di Domenico, V. Manfredi, M. Terrenzi, G. Camata, F. Mollaioli, F. Noto, P. Ricci, P. Franchin, A. Masi, E. Spacone, G.M. Verderame. Modelling and Seismic Response Analysis of Italian Pre-Code and Low-Code Reinforced Concrete Buildings. Part I: Bare Frames, y*Journal of Earthquake Engineering*, 27:6, 1482-1513, DOI: 10.1080/13632469.2022.2074919, 2023.

[11] I. Koutromanos, M. Kyriakides, A. Stavridis, Shake-table tests of a 3-story masonry-infilled RC frame retrofitted with composite materials, *Journal of Structural Engineering*, 139(8), https://doi.org/10.1061/(ASCE)ST.1943-541X.0000689, 2013.

[12] M.T. De Risi, C. Del Gaudio, S.A. Scala, G.M. Verderame, Seismic retrofitting strategies for pre-70 RC buildings: the effectiveness of "local interventions", *Procedia Structural Integrity*, 44, 958-965, https://doi.org/10.1016/j.prostr.2023.01.124, 2023.

[13] M.K. Askar, A.F. Hassan, Y.S.S. Al-Kamaki, Flexural and shear strengthening of reinforced concrete beams using FRP composites: A state of the art, *Case Studies in Construction Materials*, 17, https://doi.org/10.1016/j.cscm.2022.e01189, 2022.

[14] S. Bahji, S. Omary, V. Steiner, F. Feugeas, Strengthening reinforced concrete beams by using different types and methods of fiber-reinforces polymers: a critical review, *Practice Periodical on Structural Design and Construction*, 27(4), 2022.

[15] H. Huang, M. Guo, W. Zhang, M. Huang, Seismic behavior of strengthened RC columns under combined loadings, *Journal of Bridge Engineering,* 27(6), 2022.

[16] K. Samy, M.A. Fouda, A. Fawzy, T. Elsayed, Enhancing the Effectiveness of Strengthening RC columns with CFRP sheets, *Case Studies in Construction Materials*, 17, https://doi.org/10.1016/j.cscm.2022.e01588, 2022.

[17] M. Elsayed, B.A. Tayeh, M.A. Elmaaty, Y. Aldahshoory, Behaviour of RC columns strengthened with Ultra-High Performance Fiber Reinforced concrete (UHPFRC) under eccentric loading, *Journal of Building Engineering*, 47, 103857, https://doi.org/10.1016/j.jobe.2021.103857, 2022.

[18] S. Pampanin, G.M. Calvi, M. Moratti, Seismic Behaviour of R.C. beam-column joints designed for gravity loads, *Proc. 12th European Conference on Earthquake Engineering*, London, United Kingdom, September 9-13, 2002

[19] M.T. De Risi, P. Ricci, G.M. Verderame, G. Manfredi, Experimental assessment of unreinforced exterior beam–column joints with deformed bars, *Engineering Structures,* 112: 215-232, https://doi.org/10.1016/j.engstruct.2016.01.016, 2016.

[20] G.M. Calvi, D. Bolognini. Seismic response of reinforced concrete frames inflled with weakly reinforced masonry panels. *Journal of Earthquake Engineering*, 5:153–185. https://doi.org/10.1080/13632460109350390, 2001.

[21] P. Ezzatfar, B. Binici, Ö. Kurç, E. Canbay, H. Sucuoğlu, G. Özcebe. Application of Mesh Reinforced Mortar for Performance Enhancement of Hollow Clay Tile Infill Walls. *In: Ilki, A., Fardis, M. (eds) Seismic Evaluation and Rehabilitation of Structures. Geotechnical, Geological and Earthquake Engineering*, vol. 26. Springer, Cham. https://doi.org/10.1007/978-3-319-00458-7_10, 2014.

[22] A. Furtado, H. Rodrigues, A. Arêde, H. Varum, Out-of-plane behavior of masonry infilled RC frames based on the experimental tests available: A systematic review, *Construction and Building Materials*, 168, 831-848, https://doi.org/10.1016/j.conbuildmat.2018.02.129, 2018.

[23] L.N. Koutas, Z. Tetta, D.A. Bournas, T.C. Triantafillou, Strengthening of Concrete Structures with Textile Reinforced Mortars: State-of-the-Art Review, *Journal of Composites for Construction*, 23(1), 2019.

[24] M. Minotto, N. Verlato, M. Donà, F. da Porto, Strengthening of In-Plane and Out-of-Plane Capacity of Thin Clay Masonry Infills Using Textile- and Fiber-Reinforced Mortar, *Journal of Composites for Construction,* 24(6), 2020.

[25] A. Furtado, H. Rodrigues, A. Arêde, H. Varum, Experimental tests on strengthening strategies for masonry infill walls: A literature review, *Construction and Building Materials*, 263, 120520, https://doi.org/10.1016/j.conbuildmat.2020.120520, 2020.

[26] M.T. De Risi, A. Furtado, H. Rodrigues, J. Melo, G.M. Verderame, A. Arêde, H. Varum, G. Manfredi, Influence of textile reinforced mortars strengthening on the in-plane/out-of-plane response of masonry infill walls in RC frames, *Engineering Structures*, 254, 113887, https://doi.org/10.1016/j.engstruct.2022.113887, 2022.

[27] R. R. Milanesi, P. Morandi, C. F. Manzini, L. Albanesi, G. Magenes. Out-of-plane Response of an Innovative Masonry Infill with Sliding Joints from Shaking Table Tests, *Journal of Earthquake Engineering*, 26:4, 1789-1823, DOI: 10.1080/13632469.2020.1739173, 2022.

[28] M. Kurukulasuriya, R.R. Milanesi, G. Magenes, D. Bolognini, L. Grottoli, F. Dacarro, P. Morandi. Investigation of seismic behaviour of existing masonry infills through com-

bined cyclic in-plane and dynamic out-of-plane tests, *Proc. COMPDYN 2023,* June 12-14, 2023.

[29] G. Rebecchi, P.M. Calvi, A. Bussini, F. Dacarro, D. Bolognini, L. Grottoli, M. Rosti, F. Ripamonti, S. Cii. Full-Scale Shake Table Tests of a Reinforced Concrete Building Equipped with a Novel Servo-Hydraulic Active Mass Damper. *Journal of Earthquake Engineering*, pp.1-24, 2022.